

pubs.acs.org/macroletters Viewpoint

100th Anniversary of Macromolecular Science Viewpoint: Integrated Membrane Systems

John R. Hoffman and William A. Phillip*



Cite This: ACS Macro Lett. 2020, 9, 1267–1279



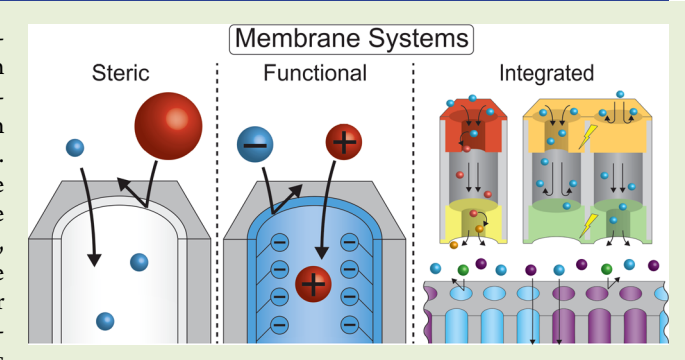
ACCESS

III Metrics & More

Article Recommendations

Supporting Information

ABSTRACT: Membranes fabricated from self-assembled materials are one recent example of how polymer science has been leveraged to advance membrane technology. Due to their well-defined nanostructures, the performance of membranes made from these materials is pushing the boundaries of size-selective filtration. Still, there remains a need for higher performance and more selective membranes. The advent of functional membrane platforms that rely on mechanisms beyond steric hindrance (e.g., charge-selective membranes and membrane sorbents) is one approach to realize improved solute—solute selectivity and further advance membrane technology. To date, the lab-scale demonstration of these platforms has often relied on fabrication schemes



that require extended processing times. However, in order to translate lab-scale demonstrations to larger-scale implementation, it is critical that the rate of the functionalization scheme is reconciled with membrane manufacturing rates. In this viewpoint, it is postulated that substrates lined by reactive moieties that are amenable to postfabrication modification would enable the production of membranes with controlled nanostructures while providing access to a diverse array of pore wall chemistries. A comparison of reaction and manufacturing rates suggests that mechanisms that exhibit second-order reaction rate constants of at least 1 M⁻¹ s⁻¹ are needed for roll-to-roll processing. Furthermore, for mechanisms that exhibit rate constants greater than 300 M⁻¹ s⁻¹, it may be possible to integrate multiple functional domains over the membrane surface such that useful properties emerge. These multifunctional systems can expand the capabilities of membranes when the patterned chemistries interact at the heterojunctions between domains (e.g., Janus and charge-patterned mosaic membranes) or if they exhibit cooperative responses to external operating conditions (e.g., membrane pumps).

1. INTRODUCTION

The fundamental scientific principles that describe transport through membranes were elucidated prior to the 1900s using an array of natural membranes (e.g., animal bladders and sausage casings). The first synthetic membranes made from cellulosic polymers were reported in 1907 and commercialized for preparative laboratory applications in the 1930s. Despite the rapid growth in polymer science and engineering following 1920,³ the application of membranes remained limited, with cellulosic derivatives dominating a small market focused on labscale and dialytic applications, until the 1960s when the nonsolvent-induced phase separation (NIPS) technique was first codified.4,5 Since that report, polymer science and membrane technology have advanced in tandem, resulting in the development of dense gas separation and reverse osmosis membranes as well as porous nanofiltration (NF), ultrafiltration (UF), and microfiltration (MF) membranes that enable an array of critical applications. For example, membranes are now routinely used to produce fresh water from seawater,6,7 separate oxygen from air, 8,9 and to clear uremic toxins from the bloodstream of patients with kidney disorders. 10 As the need for cost-effective pharmaceutical purification processes, 11,12 alternatives to energetically demanding chemical separations, ^{13,14} and the treatment of water suitable for human consumption ^{15,16} and industrial applications increases, ¹⁷ polymer membranes offer a unique and compelling means for addressing the demands of our growing global society.

The continued development of membranes requires that inherent materials design and practical engineering challenges (e.g., membrane fouling, material resiliency, and end-of-use recycling) be addressed. Among these issues, the permeability—selectivity trade-off is paramount because it dictates the nature of the solutes that can be resolved and has direct implications on the process systems that are designed around a membrane. For NF and UF membranes (pore diameters: 2—100 nm), the permeability—selectivity trade-offs arise due to the

Received: June 30, 2020 Accepted: August 12, 2020 Published: August 18, 2020





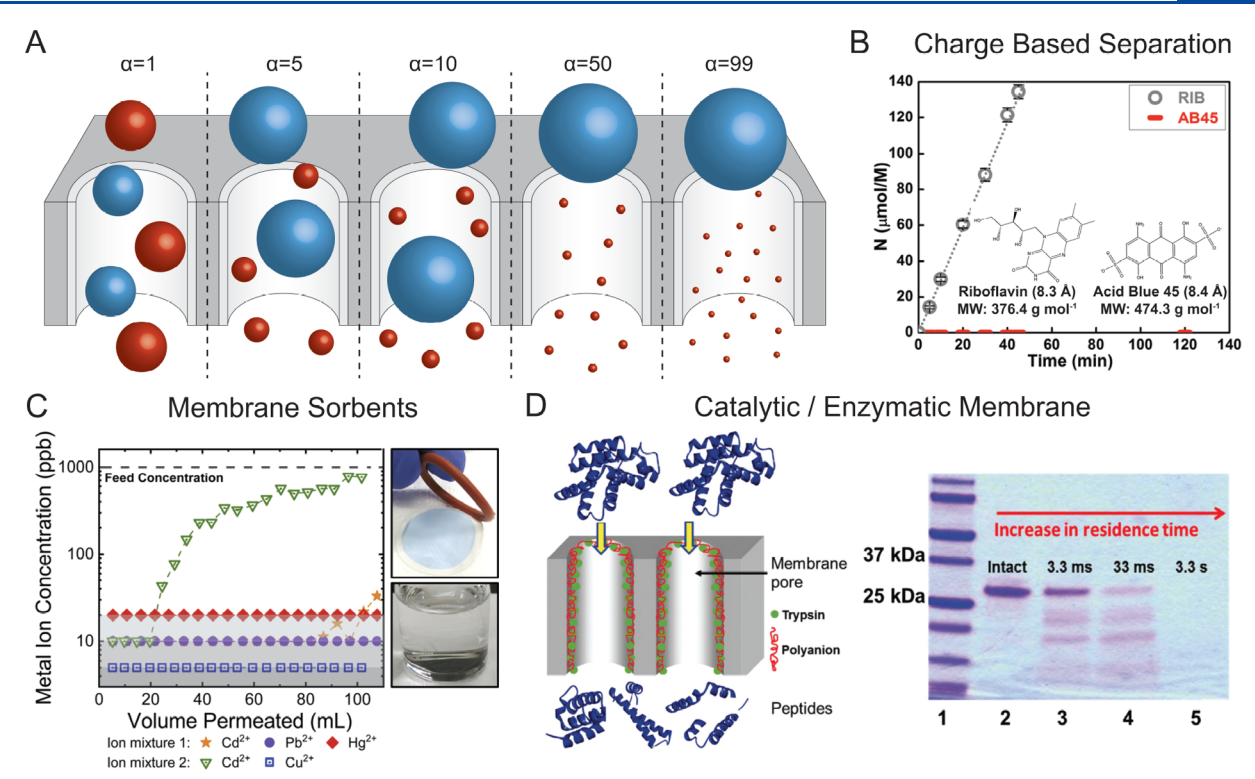


Figure 1. (A) Image (drawn to scale) demonstrating the differences in solute (red and blue spheres) and pore diameters necessary to achieve varying levels of selectivity, α, through a size-based filtration mechanism. (B) The separation of two similarly sized molecules, Riboflavin (RIB) and Acid Blue 45 (AB45), by a carboxylic acid-functionalized NF membrane (pore diameter: ~4 nm). The slope of the line through the data is proportional to the solute permeability. Thus, the large slope for Riboflavin is consistent with it being transported rapidly through the membrane, and the slope near 0 for Acid Blue 45 indicates it does not permeate through the membrane to an appreciable extent. Reprinted with permission from ref 45. Copyright 2018 American Chemical Society. (C) An adsorptive membrane for the removal of heavy metal ions. Membranes functionalized with terpyridine moieties were capable of the high affinity capture of Cd^{2+} , Pb^{2+} , and Hg^{2+} ions, from a mixed feed solution. No breakthrough of ions was observed after 100 mL of this solution permeated the membrane. These membranes were especially efficient at capturing Cu^{2+} as demonstrated by the surface of the membrane, which appeared blue, following the permeation of 100 mL of a mixed feed solution containing 1 ppm each of Cu^{2+} and Cd^{2+} ions through the membrane sorbent. Reprinted with permission from ref 69. Copyright 2018 American Chemical Society. (D) A reactive membrane for the controlled proteolysis of proteins into peptides. The enzyme trypsin, which facilitates the breakdown of proteins, is immobilized on a microporous nylon membrane. Proteins are digested as they pass through the membrane. Based on Coomassie stain analysis, increased digestion was observed at longer residence times. Namely, the signal for the intact protein is reduced, and molecules further down on the protein ladder are observed at longer residence times. Residence time was modulated by varying the flow rate through the membrane. Reprinted with permission

relationship between the membrane nanostructures and the size-selective transport mechanisms underlying their separation capabilities. 20,21 As a result of these interrelationships, increases in permeability often result in a reduction in selectivity and vice versa. Membrane throughput can be increased without sacrificing selectivity by fabricating membranes from materials that assemble into nanostructures with a high density of pores and a narrow pore size distribution (e.g., liquid crystals, ²² block polymers, ²³ membrane proteins, ²⁴ and surfactants ²⁵). ²⁶ Fundamental advances are still required to realize the potential of membranes made using these materials at larger scales. For example, even though it is a state-of-the-art membrane manufacturing process, the NIPS process is not fully understood for homopolymer systems. 5,27,28 Furthermore, the nanostructural evolution of membranes made from self-assembled materials, which are often being processed far from equilibrium, are yet to be elucidated fully. ^{29–31} Nevertheless, the ability of these approaches to increase throughput while maintaining a high selectivity has been demonstrated on the lab scale. 23-25,32,33

More selective membranes, 19,34 on the other hand, have greater potential for advancing membrane separations, but

structural advances alone are not sufficient to meet the demands of these challenging processes. Self-assembled materials are pushing the precision of size-selective filtration to its limits, such that the recovery and concentration of one solute can be achieved with an appropriately sized pore. However, the limitations of steric exclusion begin to take shape when attempting to purify solutes of similar molecular sizes. These constraints are illustrated by Figure 1A, which provides a scale representation of the size differences required to achieve separations at varying levels of selectivity. The sizes of the pore and solutes were determined by accounting for excluded volume effects at the pore mouth, 21 as shown in the Supporting Information. Here, the calculations were developed to promote the throughput of the smaller solute. For a selectivity of 10, the rejection of the red solute could be 9.1%, while the rejection of the blue solute is 91%. In order to achieve this rejection profile, the diameter of the blue solute must be 4.9× larger than that of the red solute. The difference in diameter between the two solutes can be decreased, though this requires an increase in the rejection of the target solute. For example, a selectivity of 10 can also be achieved if the rejections of the red and blue solutes are 90% and 99%, respectively. This separation could be done if

there was a 1.2× difference in solute diameters; however, only 10% of the desired product would be recovered. These calculations provide a rationale for why size-selective filtrations can be used to effect clean separations between molecules with an order of magnitude difference in molar mass but otherwise struggle. As such, developing methods for increasing selectivity while maintaining permeability will likely necessitate that the membrane chemistry is tailored to accomplish the desired separation.³⁵

Materials with controlled functionality provide avenues for developing membranes that exhibit transport properties that better mediate mass transfer and in turn provide more selective separations. Moreover, tailoring the pore wall chemistry of membranes can expand their utility beyond separations. In fact, surface modifications have already been utilized to extend the capabilities and lifetime of polymer membranes as highlighted by the examples in Figure 1.³⁶

The inclusion of functional moieties along the pore walls can lead to membranes that are capable of separating similarly sized molecules through electrostatic and van der Waals interactions.³⁵ For example, ion exchange and charge-functionalized NF membranes³⁷ use the electrostatic repulsion between likecharged entities to limit the transport of co-ions (i.e., those with the same charge as the membrane) through a Donnan exclusion mechanism.³⁸ NF membranes exploit these interactions to preferentially reject multivalent co-ions³⁹ while passing monovalent co-ions,⁴⁰ which is a useful characteristic in water-softening applications.^{41,42} Emerging membranes are enabling the selective transport of monovalent ions. For example, membranes based on metal-organic frameworks that transport F⁻ faster than Cl⁻, even though the hydrated size of F⁻ is larger than that of Cl⁻, have been reported.⁴³ This inversion in selectivity suggests that ion dehydration and membrane chemistry play a role in the underlying transport mechanism.⁴⁴ In another recent example (Figure 1B), a nanostructured, carboxylic-acid-functionalized membrane exhibited high selectivity for the transport of Riboflavin over Acid Blue 45, even though the van der Waals sizes of the molecules are within 0.1 Å of each other. 45 Beyond these examples of charge-based selectivity, the separation of neutral molecules of similar sizes is being accomplished using membranes that include other chemical features in their design. For example, the inclusion of aromatic groups can lead to membranes that mediate transport through aromaticity and $\pi - \pi$ interactions. ^{46,47} Pore walls that hydrogen bond with permeating solutes can affect transport in a similar manner. 48 Membranes modified with hydrophilic/ oleophobic surfaces find applications in oil-water separations, as the wetting characteristics that result from the surface functionality allow water to pass while retaining oil droplets.45

Porous membranes that react with the surrounding solution can be utilized as stimuli-responsive gates, as sorbents, and as high surface area supports for catalysts. For example, materials functionalized with weak polyelectrolyte brushes are often used to produce stimuli-responsive membranes. Depending upon the solution pH relative to the acid dissociation constant of the polyelectrolyte, the polymer brush will assume an extended or collapsed conformation. These conformational changes modify the effective pore size of the membrane and in turn modulate permeability. Such membranes have been utilized to act as gates for controlled release. Parameters are stimuli-responsive membranes that respond to temperature, ionic strength, light, and electric or magnetic fields have all been reported.

Membrane sorbents are lined with functional groups that selectively bind solutes. In the biopharmaceutical industry, membrane chromatography, based on these sorbents, is an established technology for the separation and purification of therapeutic proteins 53,54 as well as plasmid DNA and viruses. 55-57 In the membrane form factor, diffusion-based mass transfer limitations are reduced, allowing for membrane chromatography to achieve higher convective flow rates in comparison to packed-bed columns. 12 Sorbents have also been explored for environmental applications where the removal of pollutants (e.g., heavy metal cations⁵⁸ and anions, ⁵⁹⁻⁶¹ PFAS, ⁶² and endocrine-disrupting chemicals ⁶³) and the recovery of resources (e.g., gold, 4 uranium, 65 and nutrients 66,67) are of interest. Beyond their use for separations, the sorbents can be integrated with sensing platforms. For example, membranes designed to bind uranium accelerated the preparation of samples for nuclear forensic analysis by alpha spectroscopy.⁶⁸ Additionally, sorbents functionalized with terpyridine moieties captured heavy metal ions with high affinity (Figure 1C) and simultaneously served as fluorescent probes that quantified the extent of sorbent saturation.⁶⁹

While the primary function of a membrane is to mediate transport, membrane reactors⁷⁰ that transform solutes as they permeate⁷¹ can be realized by immobilizing catalysts along the pore walls.^{72,73} These transformations include the electrochemical or biocatalytic degradation of pollutants^{74,75} and protein digestion.⁷⁶ As shown in Figure 1D, an important advantage of membrane reactors is the ability to precisely control the residence time through changes to flow rate. Enzymatic digestion of proteins allows for structural elucidation through mass spectroscopy of the resulting peptides. Complete digestion, however, results in peptides that are too small to be of much utility for the intended purpose. Membranes lined by trypsin allowed for limited digestion, resulting in larger peptides that were better suited for characterizing the protein structure.⁷⁷

The accumulation of material from natural water sources and process streams on membrane surfaces, i.e., fouling, limits throughput and reduces the lifespan of membranes. Therefore, in contrast to the examples above, antifouling membranes seek modifications that limit the nonselective interaction and adsorption of solutes on their surfaces. Design rules for materials that reduce fouling by organic macromolecules have been established, with hydrophilic surfaces that possess no net charge being successful at combating foulant adsorption. As one example, zwitterionic functionality reduces fouling through the generation of a strongly bound hydration layer while maintaining a neutral charge. Design antifouling strategies have been reported and reviewed.

A multitude of schemes have been utilized to manipulate the pore wall chemistry of membranes for the above applications. ^{36,84,85} However, the on-demand design of next-generation membranes will require controlling both their structure and chemistry. As such, developing frameworks for reliably modifying membrane chemistries while maintaining control over their nanostructures has the potential to advance membrane science. This functionalization could occur prior to fabricating the membrane through the synthesis of novel polymer chemistries that are then transformed into nanostructured thin films. However, the effort associated with developing a new casting protocol that provides control over the nanostructure each time a polymer chemistry is developed complicates this approach significantly. Therefore, we proceed

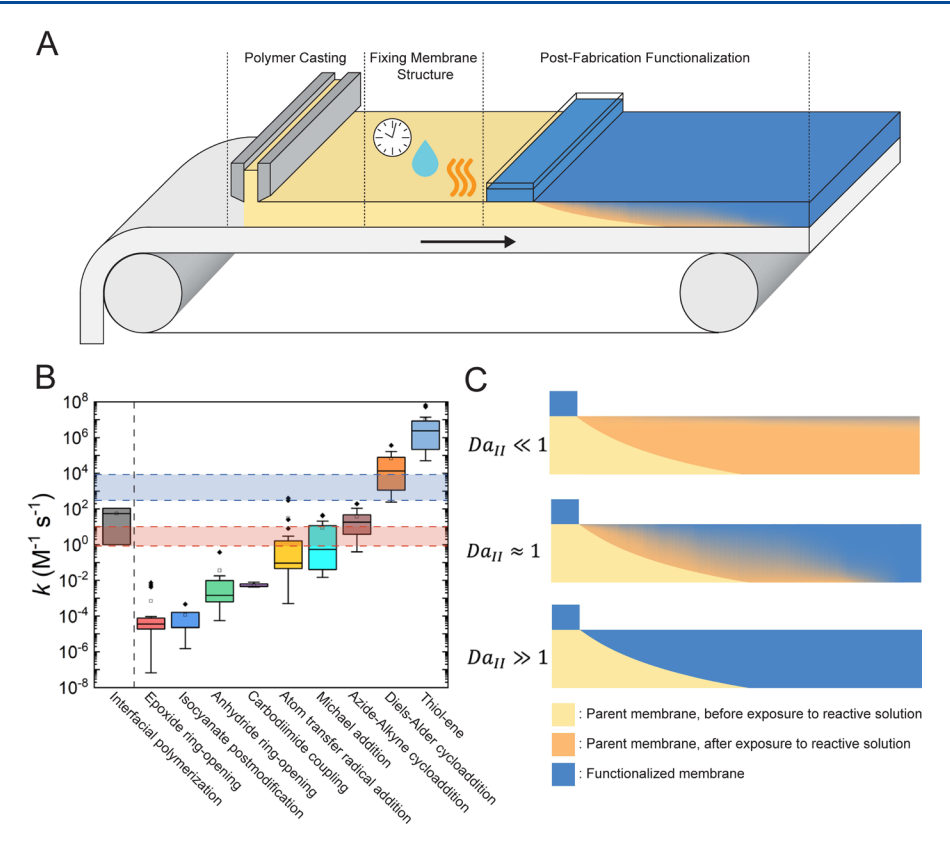


Figure 2. (A) Schematic of a membrane manufacturing process with the inclusion of a functionalization step following the fabrication of the nanostructured substrate. The substrate is formed by casting a polymer solution onto a support and inducing phase separation using a variety of processes including solvent evaporation, immersion into a nonsolvent bath, and temperature swings. (B) The reaction rate constants for nine reactions [epoxide ring opening, isocyanate postmodification, anhydride ring opening, carbodiimide coupling, atom transfer radical addition, Michael addition, azide—alkyne cycloaddition, Diels—Alder cycloaddition, and thiol—ene] are compared to those for the interfacial polymerization reactions used to fabricate desalination membranes. The band highlighted in red corresponds to the minimum reaction rate constants needed to achieve conversion at a rate that is consistent with roll-to-roll processing. The band highlighted in blue corresponds to reaction rate constants that would result in large Damköhler numbers, Da_{II} . (C) The Da_{II} compares the rate of reaction to the rate of solute transport (e.g., diffusion) within the membrane. Here, the distance the solute has diffused into the membrane is highlighted in orange, and the conversion of the coupling reaction is indicated by the blue shading. For small Da_{II} , no appreciable reaction occurs. As the Da_{II} approaches unity, conversion is determined by both the reaction and transport rates. Under these conditions, a controlled reaction front is not achieved. At large Da_{II} , the reaction is rapid, and conversion is controlled by the rate at which the reactive solutes are brought into contact. These conditions result in a reactive front that penetrates into the membrane in a consistent and controllable manner.

with the hypothesis that postfabrication functionalization processes are desirable for two reasons.

- (1) Casting protocols that produced robust substrates amenable to solid-state functionalization through reactive moieties that lined their surfaces could be developed for a smaller number of polymer systems, thereby allowing for the production of membranes with controlled nanostructures while providing access to a diverse array of pore wall chemistries.
- (2) By utilizing reactions that exhibit appropriately rapid kinetics, the functionalization processes could be controlled to integrate discrete domains of unique functionality over the membrane such that new and useful properties emerge.

This viewpoint focuses on this strategy and the novel membranes that can be produced by it. First, reaction mechanisms used for postfabrication functionalization are considered in the context of state-of-the-art membrane manufacturing processes. By comparing reaction rates to the time scale for membrane manufacturing, a range of rate constants that prove useful for roll-to-roll processing are

identified. In addition to being suitable for existing manufacturing processes, rapid reaction kinetics enable the generation of integrated membrane systems. The final section of this viewpoint surveys the current state of these multifunctional membranes and the unique properties they can exhibit.

2. REACTION RATES RELATIVE TO MEMBRANE MANUFACTURING RATES

Reconciling the rates of membrane functionalization protocols with the rates of manufacturing processes will be critical to translating lab-scale demonstration of functional membranes to larger-scale implementation (Figure 2A). In the context of the postfabrication schemes we suggest are useful, the second-order reaction rate constant is a common metric for comparing competing mechanisms. Therefore, a range of representative reaction rate constants for nine reactions that have been used to modify polymer brushes and membrane surfaces are reported in Figure 2B. A brief overview of the reactions is included within the Supporting Information. Some of the reactions [e.g., copper-catalyzed azide—alkyne cycloaddition (CuAAC)] require the use of a catalyst and are not simple second order. S8,89 For the sake of comparison, effective second-

order rate constants were evaluated at common catalyst loadings. Other considerations that will play an important role in the design of a viable processes (e.g., sensitivity to oxidants, metal-free catalysis, solvent compatibility) are not discussed. 85

The highlighted mechanisms possess representative rate

constants that span 12 orders of magnitude. In order to contemplate the kinetics that are necessary to develop functionalization protocols consistent with membrane processing rates, the reaction rate constants are compared to the rate at which the solutes within the reactive solution and the moieties on the pore wall are brought into contact. The moieties fixed to the pore wall are immobile. Therefore, the Damköhler number, $Da_{II} = \frac{kcl^2}{D}$, where k is the second-order reaction rate constant, cthe concentration of solute, l the membrane thickness, and D the diffusion coefficient of the solute in the membrane, facilitates this comparison. Figure 2C depicts the relative rates of the solute diffusion and conversion as a function of Da_{II} . For low Damköhler numbers, solute diffuses into the membrane, but the slow reaction rate results in minimal conversion being observed on relevant time scales. For $Da_{II} \sim 1$, conversion occurs but lags behind the rate at which solute is transported into the membrane. As such, additional context (i.e., the contact time between the membrane and solution) is necessary to contemplate the conditions needed to functionalize the membrane fully. For roll-to-roll manufacturing operating at a translation velocity of 5 m min⁻¹, exposing a parent membrane substrate to a reactive solution bath that is 10 m long would require conversion to be achieved in 2 min. Further assuming that the membrane and reactive solution were well-mixed (i.e., no mass transfer limitations) and the two reactants had initial concentrations of 1 M, reaction rate constants between at least 1 and $10\,\mathrm{M}^{-1}\,\mathrm{s}^{-1}$ would be necessary to achieve 99% conversion in the allotted exposure time (Supporting Information). These values are highlighted as the red domain within Figure 2B. This analysis was performed assuming a concentration of fixed sites of 1 M, which is consistent with the surface concentrations seen in ion-exchange membranes and membrane sorbents. 90,91 Reducing the concentration of fixed reactive sites would result in higher reaction rate constants being required.

The utility of this analysis is bolstered by comparing this highlighted range of rate constants to the rate constants for the interfacial polymerization reactions used in the fabrication of thin-film composite (TFC) membranes. These TFC membranes, used widely in commercial desalination applications, are made through the polymerization of acid chlorides and amines at the interface between two immiscible liquids. Analysis of the interfacial polymerization process has suggested that the formation of integral, tightly cross-linked polyamide networks, which make up the active layer of the TFC membrane, requires second-order reaction rate constants greater than $\sim 1 \text{ M}^{-1} \text{ s}^{-1}$, with most TFC membranes being formed using monomers that exhibit rate constants of 115 M⁻¹ s⁻¹.93 These values are consistent with the analysis presented above. As such, we suggest that membranes functionalized with a single moiety postfabrication will require reaction rates indicated by the red domain or greater.

As rapid functionalization routes that produce large Da_{II} are realized, opportunities exist for the development of multifunctional membranes that exhibit novel transport properties. Specifically, when $Da_{II} \gg 1$, the two species react almost "instantaneously" upon exposure. This situation can be used to produce a reaction front that propagates across the membrane in

a predictable manner, thereby allowing for distinct chemical domains to be localized at controlled positions over the membrane surface and cross-section. Assuming a concentration of fixed reactive sites of 1 M, a thickness of 1 μ m, and a diffusion coefficient of 1×10^{-8} cm² s⁻¹, a second-order reaction rate constant of $\sim 300 \text{ M}^{-1} \text{ s}^{-1}$ is required to produce $Da_{II} = 300.^{94} \text{ As}$ the membrane thickness decreases to 200 nm, the reaction rate constant required increases to $\sim 7500 \text{ M}^{-1} \text{ s}^{-1}$. This range of values is highlighted as the blue domain within Figure 2A. This scaling analysis demonstrates that high reaction rate constants are needed to control the resolution of functionalization on the submicron scale when manufacturing membranes. However, it also demonstrates that mechanisms that can exhibit the rapid reaction rates necessary to create multifunctional membranes do exist. In the next section, we highlight how new and useful properties can be accessed by drawing upon the library of functional chemistries that have already been developed and integrating them on parent membrane substrates.

3. MULTIFUNCTIONAL MEMBRANE SYSTEMS

Large Da_{II} reactions are one emerging method for integrating multiple discrete domains of chemical functionality on a single membrane substrate. The multifunctional membranes being considered here do not necessarily feature pores modified with copolymer or mixed polymer brushes; this topic is reviewed elsewhere. 84,95 Instead, chemical heterogeneity on larger length scales (i.e., >10 nm) is considered. The functionality can be distributed over the cross-section of the membrane, patterned laterally on its surface, or both. In all of these instances, $Da_{II} \gg 1$ conditions can enable the formation of discrete nano- through microscale domains of unique chemistry. For example, bands of functionality can be isolated at controlled depths over the thickness of a membrane by manipulating the sequence and timing of exposures to reactive solutions (Figure 3A). This approach has been demonstrated using the CuAAC mechanism where reactive solutions containing alkyne-terminated molecules were formulated to achieve $Da_{II} \gg 1$ conditions⁹⁶ and then deposited on azide-functionalized substrates to create dualfunctional fouling-resistant NF membranes. ⁹⁷ Another approach for creating membranes with functionality distributed over their cross-section relies on fabricating multilayer parent substrates whose component layers can be functionalized using orthogonal reaction mechanisms. 98,99 This approach has the added benefit of allowing for structural asymmetries to be introduced. Going forward, modification schemes based on rapid reactions can serve as a complement to other techniques for isolating domains of chemical functionality on surfaces such as chemical vapor deposition (CVD), polydopamine coatings, and photodegradation. These approaches have also been used to generate anisotropic membrane features, ¹⁰⁰ on time scales ranging from a few minutes (e.g., CVD and polydopamine coatings) ^{101–103} to a few hours (e.g., photodegradation). 104

Surface chemistries can be patterned with high resolution through microcontact printing, ¹⁰⁵ lithography, ^{106,107} and other printing processes ¹⁰⁸ (Figure 3B). Rapid reaction rates will still be needed when patterning the surface chemistry to reduce processing times, to suppress lateral diffusion of reactive species, and to control the manner in which the patterned functionality propagates into the depth of the membrane. Independent of the modification scheme utilized, the integrated membrane systems that result from these processes can exhibit novel properties (1) that occur when the isolated domains respond independently but in a coordinated manner to operating conditions that are

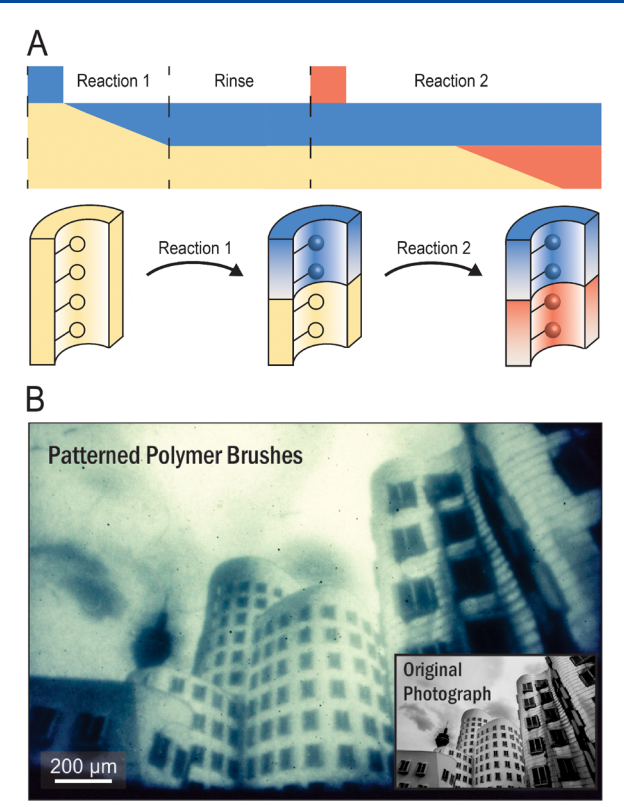


Figure 3. (A) In the $Da_{II} \gg 1$ limit, multifunctional systems can be generated by controlling the sequence and timing of exposures to reactive solutions. Using this approach, bands of functionality can be fixed at varied depths by manipulating the reaction front propagating into the membrane. Here, an example is shown where the initial solution functionalizes the upper portion of the membrane and the second solution that transforms the unreacted moieties in the underlying portion. (B) Several techniques have been developed to pattern polymer surfaces with exquisite resolution. Here, for example, surface-initiated, photoinduced electron transfer polymerization reactions were used to replicate the original photograph using polymer brushes of varying thickness. The length scale associated with this reproduction highlights the resolution to be achieved. Reprinted with permission from ref 107. Copyright 2019 American Chemical Society.

matched with natural time scales in the system or (2) which emerge due to the domains interacting with their heterojunctions.

3.1. Independent Domains and Vectorial Membrane **Transport.** MF membranes modified with functional probes already serve as components in point-of-use sensing devices such as glucose test strips. The oxidation of glucose via an immobilized enzyme generates a measurable electric response that is the basis for glucose quantification. ¹⁰⁹ The membrane in the test strip has a dual purpose, acting as a substrate for the immobilized enzyme while also screening out unwanted interactions from red blood cells and proteins. ^{110,111} DNA microarrays and multiplexed sensors ^{112,113} are examples of surfaces where patterned domains that respond independently can be used to expand on this existing role of membranes. DNA microarrays utilize immobilized probes patterned with a spacing and resolution on the order of $10-100 \mu m$ to quantify gene expression levels in a high-throughput manner. 113 The patterning isolates the probes, which helps to ensure accurate and reproducible results while making efficient use of the array size and minimizing the diffusion times to the probes. Combining these arrays with microfluidic devices leads to

sensing platforms that require smaller sample volumes, reduce costs, and provide more rapid analysis.¹¹⁴ The concept of patterned chemistries has been explored widely in the development of paper-based analytical devices (PADs).¹¹⁵ For example, bar codes, which enable the rapid, accurate, and reproducible optical detection of drugs of abuse and viral biomarkers, have been constructed using functionalized strips of paper.¹¹⁶ Polymer membranes provide access to a broader range of pore sizes than filter paper, which may provide opportunities to enhance the design of these devices while increasing the information generated through patterns. Moreover, the integration of membranes with microfluidic devices is well-established.¹¹⁷

When domains that respond independently are distributed over the membrane cross-section, there is often a need for transport to occur in a specific order and direction (vectorial membrane transport) for the desired properties to emerge. For example, natural multienzyme systems can be mimicked using immobilized enzymes¹¹⁸ arranged in the sequence needed to realize cascade reactions.¹¹⁹ This approach has been combined with the high surface area and precise residence times provided by membranes by functionalizing the upstream and downstream segments of anodic aluminum oxide (AAO) membranes with the enzymes required to execute the sequential reactions involved in the glycosyltransferase-catalyzed transglycosylation process (Figure 4). 120 When the residence time of fluid flowing through the membrane was matched with the time constant for the enzymatic reactions, the platform achieved high production efficiencies and reduced the presence of unwanted side reactions.

Multifunctional gates are another example of membranes comprised of domains that respond in independent but coordinated manners. 121 These gates are realized by functionalizing different portions of a substrate with polymer brushes that respond to the same stimulus but in different manners (e.g., a polyacid and a polybase) or by using chemistries that respond to different stimuli, such as temperature and pH. 122 When exposed to sequenced changes in stimuli, these devices have been used to mediate the transport of water, proteins, 123,124 and therapeutic drugs^{125–127} as well as to mimic ion channels.¹² The operation of a dual-stimuli responsive gate to control the transport of bovine serum albumin (BSA) is shown in Figure 5A. The leading segment of the membrane is functionalized with poly(methylacrylic acid), and the trailing segment is functionalized with poly(4-vinylpyridine) (P4VP), both of which respond to the solution pH. At pH 9, the pore entrance is closed, while the exit is open. When the pH at both ends is adjusted to pH 3, the situation reverses. The now open entrance allows the BSA to enter the pore, but the closed exit prevents the BSA from traversing the pore. Maintaining the downstream solution at pH 3 and raising the upstream solution to pH 9 sequesters the BSA in the channel of the pore. Finally, when the downstream solution is brought to pH 9, the exit opens, and BSA diffuses into the permeate stream. The effects of this sequence are observed in Figure 5B, which displays the BSA concentration versus time in the feed and permeate solutions. The influence of the sequenced pH changes is most noticeable for the permeate solution where the BSA concentration remains constant and near zero until the final step IV at which point a steady increase in concentration is observed over time. 122

Gates provide little control over the identity of the solutes being transported and cannot move solutes against their concentration gradient. Membrane pumps and ratchets, $^{129-133}$

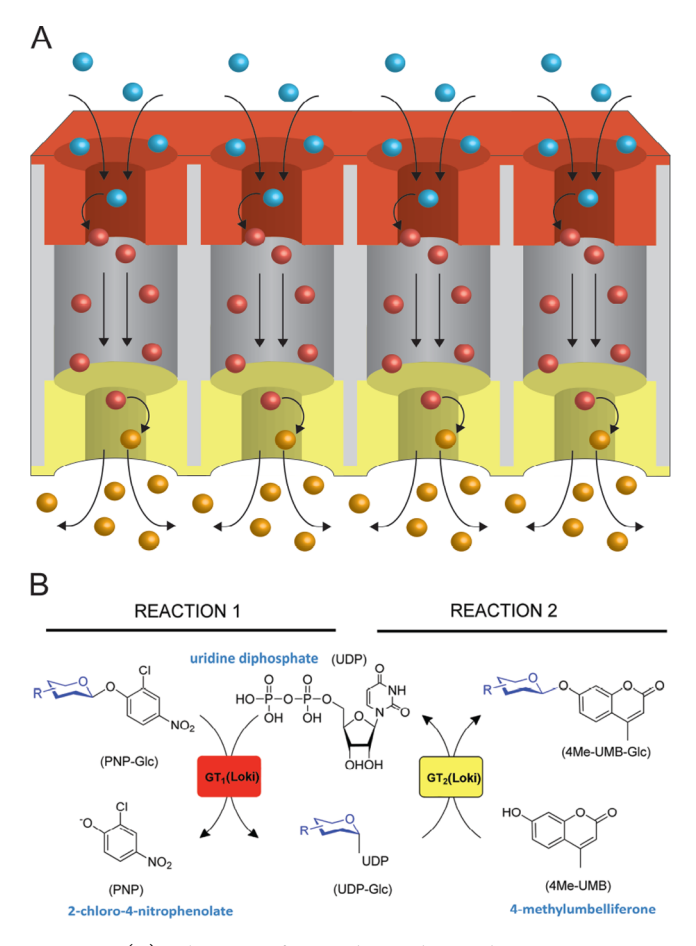


Figure 4. (A) Schematic of a membrane designed to execute a series reaction. At the leading edge, the solute is transformed to an intermediate by the first catalyst. Then, on the downstream side of the membrane the intermediate is transformed to the desired product, which passes into the permeate stream. (B) A glycosyltransferase-catalyzed transglycosylation process executed using a multifunctional membrane. A feed solution of 2-chloro-4-nitrophenyl glucose (PNP-Glc) and uridine diphosphate (UDP) is converted enzymatically to the intermediate sugar nucleotide (UDP-Glc) at the pore mouth. On the backside of the membrane, a second, distinct enzyme facilitates the formation of the product 4Me-UMB-Glc by reacting the intermediate UDP-Glc with 4-methylumbelliferone (4Me-UMB), which was introduced via a permeate sweep stream. Reprinted with permission from ref 120. Copyright 2014 American Chemical Society.

which incorporate a sorbent domain along with a responsive domain, can accomplish both of these goals. For example, membrane pumps that combined an amine-functionalized gate layer with an underlying iminodiacetic acid-functionalized sorbent layer were able to promote the transport of ions relative to neutral molecules of a comparable size when they were exposed to an oscillating pH stimulus. 129 The changing pH drove changes in the gate layer permeability and sorbent binding affinity that resulted in the enhanced transport of ions. Specifically, at high pH, the amines were deprotonated and allowed ions to diffuse to the sorbent where they were captured. When the pH decreased, the functional groups in both layers become protonated, resulting in the gate layer becoming impermeable and the ions being released from the sorbent. This combination resulted in the free ions being directed to permeate into the product stream. By oscillating the pH of the feed solution at the appropriate frequency and duty cycle, the transport of ions was enhanced relative to diffusive transport at

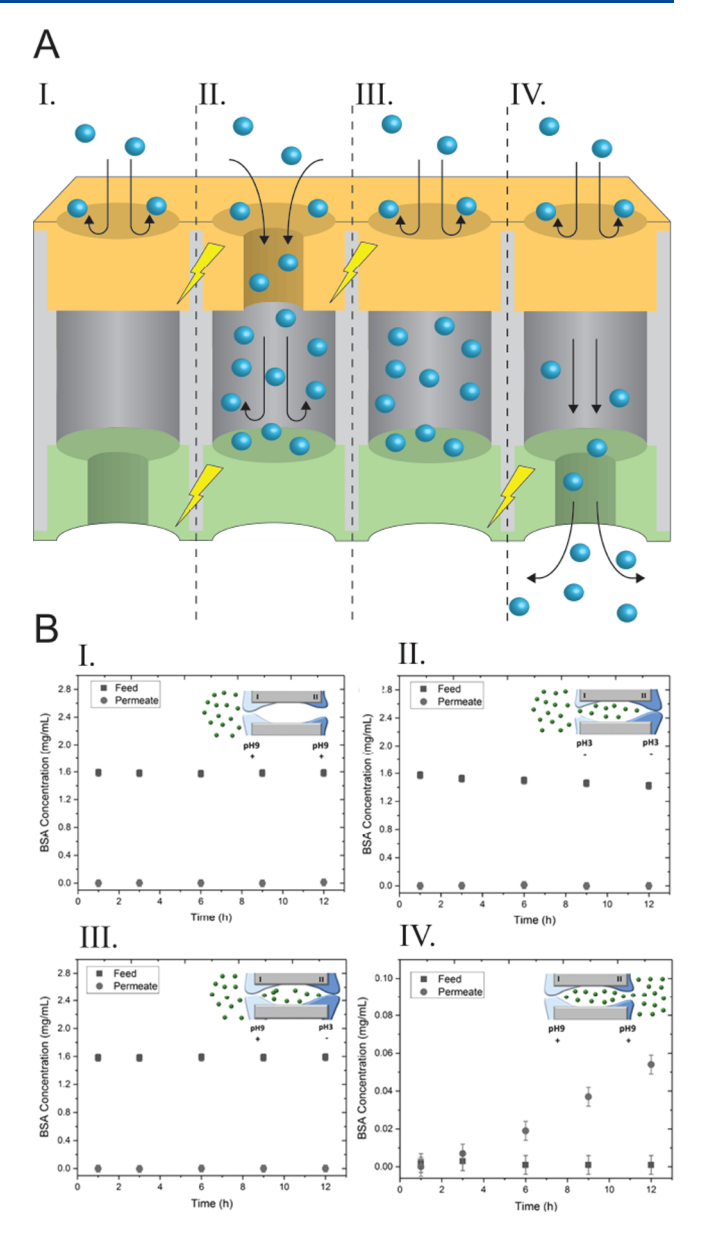


Figure 5. (A) Schematic of a dual-stimuli-responsive gate. (I) The pore entrance is closed, and no solute permeates into the membrane. (II) A stimulus causes the pore entrance to open and the exit to close, and solute enters the channel of the pore and is stopped. (III) A stimulus causes the entrance of the pore to close; no further solute enters the membrane; and the solute is trapped within the pore. (IV) The pore exit is opened, and the solute within the membrane is released into the permeate stream. (B) Experimental result for this class of membrane. The controlled transport of a protein, BSA, was achieved through the coordinated opening and closing of pH-responsive gates at the pore entrance and exit as detailed in steps I—IV. The slope of a line through the data is proportional to the solute flux. Reprinted with permission from ref 124. Copyright 2019 Elsevier B.V.

constant pH. The function of these pumps may be enhanced by developing component layers that respond more selectively. For example, a switch that only becomes activated when a specific molecule is present can be included within the membrane. AAO membranes lined by poly[(N-isopropylacrlyamide-co-4(3-acryloylthioereido) benzoic acid) $_{0.2}$] copolymer brushes, which formed a dynamic bond with inositol phosphate to close the pores, are one example of this approach. ¹³⁴ Moving forward, control over structure and chemistry at multiple length scales

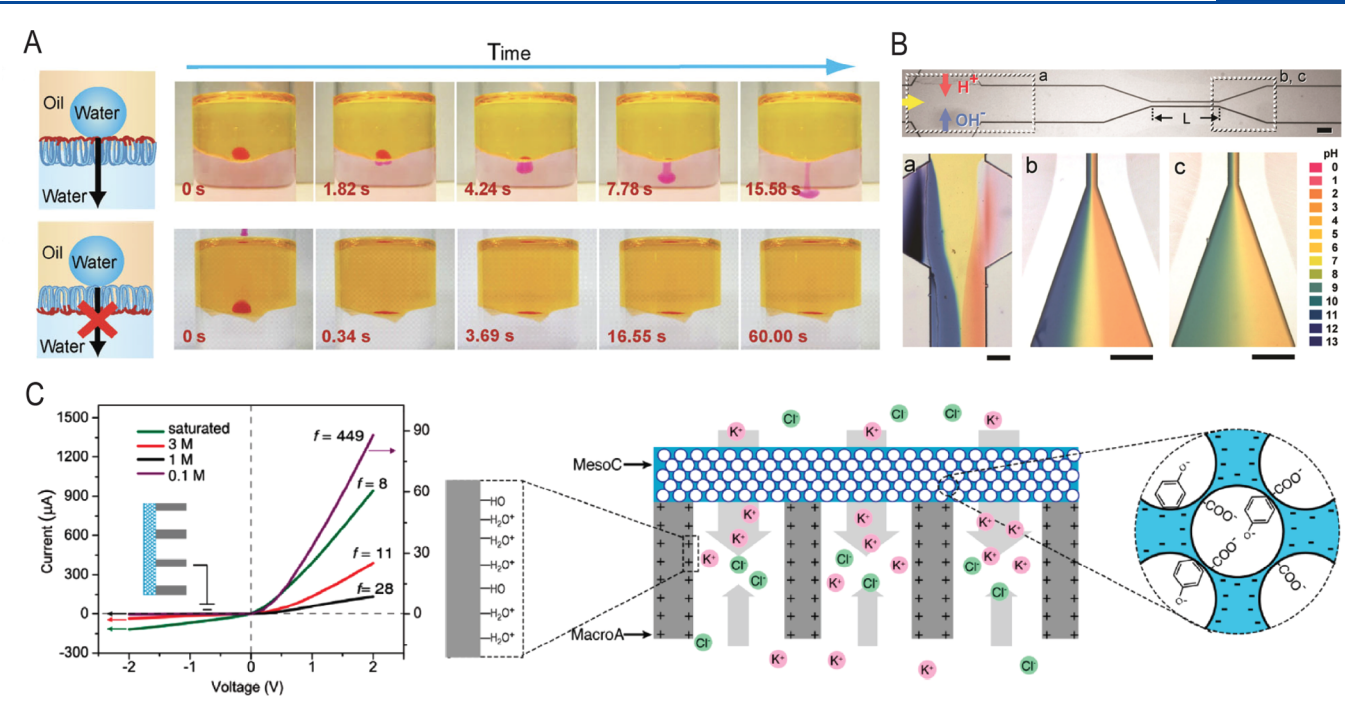


Figure 6. (A) Hydropholic Janus membrane exhibits directional permeation of water. When a water droplet (dyed red) is placed upon the hydrophobic side of the membrane (thin red layer), it exerts a large Laplace pressure, creating a driving force for its permeation across the interface. When the droplet is placed on the hydropholic side of the membrane (thick blue layer), it spreads out, resulting in a Laplace pressure that is insufficient to drive the droplet across the hydrophobic barrier. Reprinted with permission from ref 101. Copyright 2014 John Wiley and Sons. (B) Bipolar membranes coupled with a microfluidic device for the creation of stable pH variations. Protons and hydroxide ions are formed through two bipolar membranes at the entrance of the microfluidic channel (subset a). The indicator color reports the local pH. The length of a narrow constriction in the channel downstream of the membranes controls mixing to generate pH gradients. A short channel (subset b) results in sharper interfaces and larger gradients, while a long channel (subset c) results in more gradual variations. Reprinted with permission from ref 137. Copyright 2011 AIP Publishing. (C) Ionic diodes made from membranes with structural and chemical asymmetries. Current—voltage (I-V) curves, which show near zero current at negative applied biases and high current at positive applied biases, demonstrate that the high ion rectification ratio persists over a wide range of salt concentrations. This behavior is driven by the preferential flow of K^+ ions through the negatively charged mesoporous carbon layer. Reprinted with permission from ref 151. Copyright 2014 American Chemical Society.

could be leveraged to produce polymer membranes that better mimicked the functions of biological membranes.

3.2. Transport Properties that Emerge due to Interactions at Heterojunctions. The examples highlighted above describe properties that arise through the cooperative response of independent domains. Useful properties can also be accessed when domains interact at their heterojunctions. In these instances, the interactions, which are often driven by the opposing characteristics of the domains (e.g., hydrophobic and hydrophilic, positively charged and negatively charged), lead to changes in the local energetic landscape that affect transport.

Janus membranes, 100,135,136 for example, are characterized by their antipodal segments being functionalized with chemistries that possess asymmetric properties. ¹³⁵ The interactions between these layers create an internal driving force that has a preferred orientation, which is aligned perpendicular to the thin dimension of the membrane. Therefore, the transport properties of Janus membranes depend on the direction in which external driving forces are applied. For example, water diodes can be generated using membranes composed of a hydrophobic and a hydrophilic layer (Figure 6A). When the hydrophobic layer faces a feed solution containing water droplets suspended in oil, the surface tension of the droplet generates a large pressure that drives its permeation through the membrane. The water droplet does not permeate when the membrane is situated in the reverse orientation. Instead, the droplet spreads out over the hydrophilic surface, reducing the pressure it experiences. Along with the

directional permeation of water, Janus membranes exhibit several other intriguing properties related to multiphase flows that could find application in air sparging, triphasic reactors, and fog-harvesting processes. These development efforts are identifying how the structuring of the chemical heterogeneity influences performance. For example, in the forward orientation, the thickness of the hydrophobic layer dominates the applied pressure needed to drive the transport of water while the hydrophilic layer thickness has little impact. ^{101,135} Observations such as this one demonstrate the need to develop modification schemes, such as those discussed in Section 2, that provide high fidelity control over the distribution of the chemical functionality that is introduced.

Bipolar membranes, consisting of anion-selective and cation-selective domains, are another class of Janus membrane. When operated with a forward bias, i.e., the applied voltage relative to the membrane orientation is in the direction of easy current flow, counterions move toward the heterojunction, and the system exhibits an increasingly conductive response. When a small reverse bias is applied, the current is carried by co-ion crossover and water dissociation, which result in a low conductance state. At large reverse bias, the magnitude of the electric field at the heterojunction interface enhances the rate of heterolytic water dissociation, resulting in the increased generation of H⁺ and OH⁻ ions. The layered bipolar structure allows these ions to permeate into the surrounding solutions through their counter-charged domain while limiting

the transport of co-ions 138 such that these membrane find use as pH actuators in microfluidic devices ¹³⁷ (Figure 6B) as well as an energy-efficient alternative to electrolysis. 138 Balancing the need to minimize the transfer of co-ions across the interface while promoting the transport of water to replace that which is dissociated remains a challenge in the design of these systems. 139,140 Bipolar membranes have been modified with layer-by-layer coatings to manage co-ion leakage 138 as well as with nanoparticles to increase the interfacial area between charged domains, which lead to increased water dissociation and reduced water depletion. However, there is still room to advance these integrated systems where control over structure and chemistry is critical. Recently, a novel use of the bipolar membrane structure attached photoacid molecules covalently at the heterojunction. Subsequently, the absorption of light by the photoacid resulted in photovoltaic action, which suggests that these multifunctional membranes could lead to devices that convert sunlight directly into ionic electricity. 143,144

Bipolar membranes can function as ionic diodes, which exhibit asymmetric current voltage curves (Figure 6C). This asymmetry indicates that there is a preferential direction for ion flow, 145 which resembles the unique properties found in biological systems such as aquaporins and ion channels. 146 Efforts to develop bioinspired membranes 147 that exhibit this behavior have identified various phenomena underlying systems that exhibit high ionic rectification. These phenomena are associated with structural and chemical asymmetries. Conical nanopores are an example of structural asymmetry, 145 while bipolar membranes¹⁴⁸ and those that have gradients in surface charge over their pore length are examples of chemical asymmetries that lead to ion rectification. Typically, these phenomena were identified by fundamental studies executed with single nanopore films, and translating them to viable, multichannel devices remains a challenge. 150 A promising example achieved this translation by layering mesoporous carbon on top of macroporous alumina. This system coupled both geometric and chemical (charge) asymmetry between the two layers such that it was able to achieve high rectification ratios even in solutions saturated with potassium chloride (Figure 6C). This type of performance has potential application in power generation through the mixing of salinity gradients 152 as well as sensing.

As these systems are developed further, the utilization of rapid, postmodification reactions offers the potential for the generation of multifunctional membranes with tailored solute interactions. For example, studies have shown in addition to the functionality within the pore that the functionality on the membrane surface results in a synergistic effect for controlling ion gating. Multifunctional membranes have been shown to improve the selectivity of nanopores, with the inclusion of crown ethers within a solid-state nanopore coupled with a DNA-functionalized surface resulting in high selectivity of potassium over sodium. This transport is controlled by the selective interactions of crown ethers with potassium, with the inclusion of DNA on the surface leading to an increase in ion concentration at the pore entrance. This type of selectivity tries to mimic the ion pumping seen in biological systems.

Finally, membranes with charge-patterned surfaces provide clear examples of how chemical heterogeneity can engender useful characteristics.⁹⁸ In electrodialysis, ion exchange membranes exhibit an Ohmic response at low applied potentials. As the potential is increased, a limiting current plateau is reached due to the depletion of charge carrying ions. At even higher

potentials, an overlimiting regime occurs where the system again exhibits an Ohmic response due to mixing engendered vortices that result from an electroconvection instability. 117 In comparison to unmodified membranes, cation exchange membranes patterned with poly(2-vinylpyridine) domains exhibited reduced limiting current plateau lengths and lower membrane resistances, as the surface topology reduced the potential necessary to produce electroconvective flow and tailored the direction of the flow toward the membrane. 156,157 In a separate series of experiments, where pressure-driven flow mediated transport, the positive and negative domains of chargepatterned mosaic membranes provided separate pathways for the coupled permeation of anions and cations. This patterning resulted in dissolved salts permeating at a rate faster than that of water, 108,158 thereby enriching the concentration of salt in the product stream. 159 Recent work examining the influence of the pattern geometry on salt transport demonstrated that membranes with higher densities of interfacial junctions exhibited high salt fluxes, which suggests that local variations in the electrical potential near the interfacial junctions are critical to the ion transport mechanism. 160 Other types of chemically patterned surfaces could allow for the interactions between membranes and solutions to be tailored precisely. 161,162 This observation could provide an avenue for manipulating the strength of the bound hydration layer that is critical to interfacial phenomena such as membrane fouling and solute partitioning.

4. CONCLUSIONS

Polymer membranes with pores lined by reactive moieties that can be molecularly engineered after the membrane nanostructure has been fixed in place can help to meet the growing demand for more selective membranes with tailor-made performance profiles. Reaction rate constants needed to manufacture such membranes at a commercial scale were identified by comparing representative reaction rates with the rate of roll-to-roll membrane processing. The versatility associated with the highlighted mechanisms suggests that the postfabrication modification of membranes can accommodate a vast array of pore wall chemistries. In addition to membranes lined by a single functional moiety, there are significant opportunities for expanding the overall capabilities of membranes through the integration and patterning of multiple functional domains on a single substrate. These integrated membrane systems are just beginning to emerge, and polymer chemists and membrane scientists will need to collaborate in order to realize the potential for them to advance membrane technology further.

ASSOCIATED CONTENT

Supporting Information

The Supporting Information is available free of charge at https://pubs.acs.org/doi/10.1021/acsmacrolett.0c00482.

Detailed calculations of selectivity as a function of pore and solute sizes, reaction rate constants needed to achieve sufficient conversion in roll-to-roll processing, reaction rate constants needed to achieve high Damköhler number, discussion, and table of reaction rate constants extracted from the literature (PDF)

AUTHOR INFORMATION

Corresponding Author

William A. Phillip — 205 McCourtney Hall, Department of Chemical and Biomolecular Engineering, University of Notre Dame, Notre Dame, Indiana 46556, United States;

orcid.org/0000-0001-8871-585X; Email: wphillip@nd.edu

Author

John R. Hoffman – 205 McCourtney Hall, Department of Chemical and Biomolecular Engineering, University of Notre Dame, Notre Dame, Indiana 46556, United States

Complete contact information is available at: https://pubs.acs.org/10.1021/acsmacrolett.0c00482

Notes

The authors declare no competing financial interest.

■ ACKNOWLEDGMENTS

This work was made possible with support from the National Science Foundation (NSF) through the Advanced Manufacturing Program (Award 1932206), and we appreciatively acknowledge this support. J.R.H. gratefully acknowledges support from the Center of Environmental Science and Technology (CEST)/Bayer Predoctoral Fellowship at the University of Notre Dame.

REFERENCES

- (1) Lonsdale, H. K. J. Membr. Sci. 1982, 10, 81-181.
- (2) Baker, R. W. Membrane Technology and Applications, 3rd ed.; John Wiley: Chichester, West Sussex, UK, 2012.
- (3) Stamm, M. Introduction to Physical Polymer Science. *Macromol. Chem. Phys.* **2006**, 207, 787–787.
- (4) Loeb, S.; Sourirajan, S. Sea Water Demineralization by Means of an Osmotic Membrane. *Adv. Chem. Ser.* **1963**, 38, 117–132.
- (5) Guillen, G. R.; Pan, Y.; Li, M.; Hoek, E. M. V. Preparation and Characterization of Membranes Formed by Nonsolvent Induced Phase Separation: A Review. *Ind. Eng. Chem. Res.* **2011**, *50*, 3798–3817.
- (6) Greenlee, L. F.; Lawler, D. F.; Freeman, B. D.; Marrot, B.; Moulin, P. Reverse Osmosis Desalination: Water Sources, Technology, and Today's Challenges. *Water Res.* **2009**, *43*, 2317–2348.
- (7) Elimelech, M.; Phillip, W. A. The Future of Seawater Desalination: Energy, Technology, and the Environment. *Science* **2011**, 333, 712–717.
- (8) Sanders, D. F.; Smith, Z. P.; Guo, R.; Robeson, L. M.; McGrath, J. E.; Paul, D. R.; Freeman, B. D. Energy-efficient Polymeric Gas Separation Membranes for a Sustainable Future: A Review. *Polymer* **2013**, *54*, 4729–4761.
- (9) Weidman, J. R.; Guo, R. The Use of Iptycenes in Rational Macromolecular Design for Gas Separation Membrane Applications. *Ind. Eng. Chem. Res.* **2017**, *56*, 4220–4236.
- (10) Ronco, C.; Clark, W. R. Haemodialysis Membranes. *Nat. Rev. Nephrol.* **2018**, *14*, 394–410.
- (11) Marchetti, P.; Jimenez Solomon, M. F.; Szekely, G.; Livingston, A. G. Molecular Separation with Organic Solvent Nanofiltration: A Critical Review. *Chem. Rev.* **2014**, *114*, 10735–10806.
- (12) van Reis, R.; Zydney, A. Bioprocess Membrane Technology. J. Membr. Sci. 2007, 297, 16–50.
- (13) Sholl, D. S.; Lively, R. P. Seven Chemical Separations to Change the World. *Nature* **2016**, 532, 435–437.
- (14) Lively, R. P.; Sholl, D. S. From Water to Organics in Membrane Separations. *Nat. Mater.* **2017**, *16*, 276–279.
- (15) Shannon, M. A.; Bohn, P. W.; Elimelech, M.; Georgiadis, J. G.; Mariñas, B. J.; Mayes, A. M. Science and Technology for Water Purification in the Coming Decades. *Nature* **2008**, *452*, 301–310.
- (16) Hering, J. G.; Waite, T. D.; Luthy, R. G.; Drewes, J. E.; Sedlak, D. L. A Changing Framework for Urban Water Systems. *Environ. Sci. Technol.* **2013**, 47, 10721–10726.

- (17) Zodrow, K. R.; Li, Q.; Buono, R. M.; Chen, W.; Daigger, G.; Dueñas-Osorio, L.; Elimelech, M.; Huang, X.; Jiang, G.; Kim, J.-H.; Logan, B. E.; Sedlak, D. L.; Westerhoff, P.; Alvarez, P. J. J. Advanced Materials, Technologies, and Complex Systems Analyses: Emerging Opportunities to Enhance Urban Water Security. *Environ. Sci. Technol.* 2017, *51*, 10274–10281.
- (18) Eugene, E. A.; Phillip, W. A.; Dowling, A. W. Data Science-enabled Molecular-to-systems Engineering for Sustainable Water Treatment. *Curr. Opin. Chem. Eng.* **2019**, *26*, 122–130.
- (19) Park, H. B.; Kamcev, J.; Robeson, L. M.; Elimelech, M.; Freeman, B. D. Maximizing the Right Stuff: The Trade-off between Membrane Permeability and Selectivity. *Science* **2017**, *356*, 1137.
- (20) Zeman, L. J.; Zydney, A. L. Microfiltration and Ultrafiltration: Principles and Applications; CRC Press: 2017.
- (21) Mehta, A.; Zydney, A. L. Permeability and Selectivity Analysis for Ultrafiltration Membranes. *J. Membr. Sci.* **2005**, 249, 245–249.
- (22) Feng, X.; Imran, Q.; Zhang, Y.; Sixdenier, L.; Lu, X.; Kaufman, G.; Gabinet, U.; Kawabata, K.; Elimelech, M.; Osuji, C. O. Precise Nanofiltration in a Fouling-resistant Self-assembled Membrane with Water-continuous Transport Pathways. *Sci. Adv.* **2019**, *5*, eaav9308.
- (23) Zhang, Y.; Mulvenna, R. A.; Qu, S.; Boudouris, B. W.; Phillip, W. A. Block Polymer Membranes Functionalized with Nanoconfined Polyelectrolyte Brushes Achieve Sub-Nanometer Selectivity. *ACS Macro Lett.* **2017**, *6*, 726–732.
- (24) Tu, Y.-M.; Song, W.; Ren, T.; Shen, Y.-X.; Chowdhury, R.; Rajapaksha, P.; Culp, T. E.; Samineni, L.; Lang, C.; Thokkadam, A.; Carson, D.; Dai, Y.; Mukthar, A.; Zhang, M.; Parshin, A.; Sloand, J. N.; Medina, S. H.; Grzelakowski, M.; Bhattacharya, D.; Phillip, W. A.; Gomez, E. D.; Hickey, R. J.; Wei, Y.; Kumar, M. Rapid Fabrication of Precise High-throughput Filters from Membrane Protein Nanosheets. *Nat. Mater.* **2020**, *19*, 347–354.
- (25) Liang, Y.; Zhu, Y.; Liu, C.; Lee, K. R.; Hung, W. S.; Wang, Z.; Li, Y.; Elimelech, M.; Jin, J.; Lin, S. Polyamide Nanofiltration Membrane with Highly Uniform Sub-nanometre Pores for Sub-1 A Precision Separation. *Nat. Commun.* **2020**, *11*, 2015.
- (26) Werber, J. R.; Osuji, C. O.; Elimelech, M. Materials for Next-generation Desalination and Water Purification Membranes. *Nat. Rev. Mater.* **2016**, *1*, 16018.
- (27) Tree, D. R.; Dos Santos, L.; Wilson, C. B.; Scott, T. R.; Garcia, J. U.; Fredrickson, G. H. Mass-transfer Driven Spinodal Decomposition in a Ternary Polymer Solution. *Soft Matter* **2019**, *15*, 4614–4628.
- (28) Tree, D. R.; Iwama, T.; Delaney, K. T.; Lee, J.; Fredrickson, G. H. Marangoni Flows during Nonsolvent Induced Phase Separation. *ACS Macro Lett.* **2018**, *7*, 582–586.
- (29) Oss-Ronen, L.; Schmidt, J.; Abetz, V.; Radulescu, A.; Cohen, Y.; Talmon, Y. Characterization of Block Copolymer Self-Assembly: From Solution to Nanoporous Membranes. *Macromolecules* **2012**, *45*, 9631–9642.
- (30) Gu, Y.; Dorin, R. M.; Tan, K. W.; Smilgies, D.-M.; Wiesner, U. In Situ Study of Evaporation-Induced Surface Structure Evolution in Asymmetric Triblock Terpolymer Membranes. *Macromolecules* **2016**, 49, 4195–4201.
- (31) Stegelmeier, C.; Exner, A.; Hauschild, S.; Filiz, V.; Perlich, J.; Roth, S. V.; Abetz, V.; Förster, S. Evaporation-Induced Block Copolymer Self-Assembly into Membranes Studied by in Situ Synchrotron SAXS. *Macromolecules* **2015**, *48*, 1524–1530.
- (32) Zhang, Y.; Sargent, J. L.; Boudouris, B. W.; Phillip, W. A. Nanoporous Membranes Generated from Self-assembled Block Polymer Precursors: Quo Vadis? *J. Appl. Polym. Sci.* **2015**, 132, 41683.
- (33) Zhang, Y.; Almodovar-Arbelo, N. E.; Weidman, J. L.; Corti, D. S.; Boudouris, B. W.; Phillip, W. A. Fit-for-purpose Block Polymer Membranes Molecularly Engineered for Water Treatment. *NPJ. Clean Water* **2018**, *1*, 1–14.
- (34) Werber, J. R.; Deshmukh, A.; Elimelech, M. The Critical Need for Increased Selectivity, Not Increased Water Permeability, for Desalination Membranes. *Environ. Sci. Technol. Lett.* **2016**, *3*, 112–120.
- (35) Sadeghi, I.; Kaner, P.; Asatekin, A. Controlling and Expanding the Selectivity of Filtration Membranes. *Chem. Mater.* **2018**, *30*, 7328–7354.

- (36) Miller, D. J.; Dreyer, D. R.; Bielawski, C. W.; Paul, D. R.; Freeman, B. D. Surface Modification of Water Purification Membranes. *Angew. Chem., Int. Ed.* **2017**, *56*, 4662–4711.
- (37) Geise, G. M. Experimental Characterization of Polymeric Membranes for Selective Ion Transport. *Curr. Opin. Chem. Eng.* **2020**, 28, 36–42.
- (38) Donnan, F. G. The Theory of Membrane Equilibria. *Chem. Rev.* **1924**, *1*, 73–90.
- (39) Yaroshchuk, A. E. Non-steric Mechanisms of Nanofiltration: Superposition of Donnan and Dielectric Exclusion. *Sep. Purif. Technol.* **2001**, *22*, 143–158.
- (40) Luo, J.; Wan, Y. Effects of pH and Salt on Nanofiltration—A Critical Review. J. Membr. Sci. 2013, 438, 18–28.
- (41) Van Der Bruggen, B.; Vandecasteele, C. Removal of Pollutants from Surface Water and Groundwater by Nanofiltration: Overview of Possible Applications in the Drinking Water Industry. *Environ. Pollut.* **2003**, *122*, 435–445.
- (42) Ouyang, L.; Malaisamy, R.; Bruening, M. L. Multilayer Polyelectrolyte Films as Nanofiltration Membranes for Separating Monovalent and Divalent Cations. *J. Membr. Sci.* **2008**, *310*, 76–84.
- (43) Li, X.; Zhang, H.; Wang, P.; Hou, J.; Lu, J.; Easton, C. D.; Zhang, X.; Hill, M. R.; Thornton, A. W.; Liu, J. Z.; Freeman, B. D.; Hill, A. J.; Jiang, L.; Wang, H. Fast and Selective Fluoride Ion Conduction in Sub-1-nanometer Metal-organic Framework Channels. *Nat. Commun.* **2019**, 10, 2490.
- (44) Zhang, H.; Hou, J.; Hu, Y.; Wang, P.; Ou, R.; Jiang, L.; Liu, J. Z.; Freeman, B. D.; Hill, A. J.; Wang, H. Ultrafast Selective Transport of Alkali Metal Ions in Metal Organic Frameworks with Subnanometer Pores. *Sci. Adv.* **2018**, *4*, No. eaaq0066.
- (45) Sadeghi, I.; Kronenberg, J.; Asatekin, A. Selective Transport through Membranes with Charged Nanochannels Formed by Scalable Self-Assembly of Random Copolymer Micelles. *ACS Nano* **2018**, *12*, 95–108.
- (46) Sadeghi, I.; Asatekin, A. Membranes with Functionalized Nanopores for Aromaticity-Based Separation of Small Molecules. *ACS Appl. Mater. Interfaces* **2019**, *11*, 12854–12862.
- (47) Kamaz, M.; Sengupta, A.; Depaz, S. S.; Chiao, Y.-H.; Ranil Wickramasinghe, S. Poly(ionic liquid) Augmented Membranes for π Electron Induced Separation/fractionation of Aromatics. *J. Membr. Sci.* **2019**, *579*, 102–110.
- (48) Bush, A. M.; Ford, H. O.; Gao, F.; Summe, M. J.; Rouvimov, S.; Schaefer, J. L.; Phillip, W. A.; Guo, R. Tunable Mesoporous Films from Copolymers with Degradable Side Chains as Membrane Precursors. *J. Membr. Sci.* **2018**, *567*, 104–114.
- (49) Wang, Y.; Gong, X. Special Oleophobic and Hydrophilic Surfaces: Approaches, Mechanisms, and Applications. *J. Mater. Chem. A* **2017**, *5*, 3759–3773.
- (50) Wandera, D.; Wickramasinghe, S. R.; Husson, S. M. Stimuli-responsive Membranes. *J. Membr. Sci.* **2010**, *357*, 6–35.
- (51) Stuart, M. A. C.; Huck, W. T. S.; Genzer, J.; Muller, M.; Ober, C.; Stamm, M.; Sukhorukov, G. B.; Szleifer, I.; Tsukruk, V. V.; Urban, M.; Winnik, F.; Zauscher, S.; Luzinov, I.; Minko, S. Emerging Applications of Stimuli-responsive Polymer Materials. *Nat. Mater.* **2010**, *9*, 101–113.
- (52) Zhang, K.; Wu, X. Y. Temperature and pH-responsive Polymeric Composite Membranes for Controlled Delivery of Proteins and Peptides. *Biomaterials* **2004**, *25*, 5281–5291.
- (53) Ghosh, R. Protein Separation using Membrane Chromatography: Opportunities and Challenges. *J. Chromatogr. A* **2002**, 952, 13–27.
- (54) van Reis, R.; Zydney, A. Membrane Separations in Biotechnology. *Curr. Opin. Biotechnol.* **2001**, *12*, 208–211.
- (55) Orr, V.; Zhong, L.; Moo-Young, M.; Chou, C. P. Recent Advances in Bioprocessing Application of Membrane Chromatography. *Biotechnol. Adv.* **2013**, *31*, 450–465.
- (56) Boi, C. Membrane Adsorbers as Purification Tools for Monoclonal Antibody Purification. *J. Chromatogr. B: Anal. Technol. Biomed. Life Sci.* **2007**, 848, 19–27.
- (57) Liu, W.; Bennett, A. L.; Ning, W.; Tan, H.-Y.; Berwanger, J. D.; Zeng, X.; Bruening, M. L. Monoclonal Antibody Capture and Analysis

- Using Porous Membranes Containing Immobilized Peptide Mimotopes. *Anal. Chem.* **2018**, *90*, 12161–12167.
- (58) Mulchandani, A.; Westerhoff, P. Recovery Opportunities for Metals and Energy from Sewage Sludges. *Bioresour. Technol.* **2016**, 215, 215–226.
- (59) Liu, B.; Kim, K.-H.; Kumar, V.; Kim, S. A Review of Functional Sorbents for Adsorptive Removal of Arsenic Ions in Aqueous Systems. *J. Hazard. Mater.* **2020**, 388, 121815.
- (60) Cumbal, L.; Sengupta, A. K. Arsenic Removal Using Polymer-supported Hydrated Iron(III) Oxide Nanoparticles: Role of Donnan Membrane Effect. *Environ. Sci. Technol.* **2005**, *39*, 6508–6515.
- (61) Gifford, M.; Hristovski, K.; Westerhoff, P. Ranking Traditional and Nano-enabled Sorbents for Simultaneous Removal of Arsenic and Chromium from Simulated Groundwater. *Sci. Total Environ.* **2017**, 601–602, 1008–1014.
- (62) Kumarasamy, E.; Manning, I. M.; Collins, L. B.; Coronell, O.; Leibfarth, F. A. Ionic Fluorogels for Remediation of Per- and Polyfluorinated Alkyl Substances from Water. *ACS Cent. Sci.* **2020**, *6*, 487–492.
- (63) Alsbaiee, A.; Smith, B. J.; Xiao, L.; Ling, Y.; Helbling, D. E.; Dichtel, W. R. Rapid Removal of Organic Micropollutants from Water by a Porous β -cyclodextrin Polymer. *Nature* **2016**, *529*, 190.
- (64) Villalobos, L. F.; Yapici, T.; Peinemann, K.-V. Polythiosemicarbazide Membrane for Gold Recovery. *Sep. Purif. Technol.* **2014**, *136*, 94–104.
- (65) Liu, C.; Hsu, P.-C.; Xie, J.; Zhao, J.; Wu, T.; Wang, H.; Liu, W.; Zhang, J.; Chu, S.; Cui, Y. A Half-wave Rectified Alternating Current Electrochemical Method for Uranium Extraction from Seawater. *Nat. Energy* **2017**, *2*, 17007.
- (66) Tarpeh, W. A.; Udert, K. M.; Nelson, K. L. Comparing Ion Exchange Adsorbents for Nitrogen Recovery from Source-Separated Urine. *Environ. Sci. Technol.* **2017**, *51*, 2373–2381.
- (67) Clark, B.; Tarpeh, W. A. Selective Recovery of Ammonia Nitrogen from Wastewaters with Transition Metal-loaded Polymeric Cation Exchange Adsorbents. *Chem. Eur. J.* **2020**, *26*, 10099.
- (68) Duval, C. E.; Darge, A. W.; Ruff, C.; DeVol, T. A.; Husson, S. M. Rapid Sample Preparation for Alpha Spectroscopy with Ultrafiltration Membranes. *Anal. Chem.* **2018**, *90*, 4144–4149.
- (69) Zhang, Y.; Vallin, J. R.; Sahoo, J. K.; Gao, F.; Boudouris, B. W.; Webber, M. J.; Phillip, W. A. High-Affinity Detection and Capture of Heavy Metal Contaminants using Block Polymer Composite Membranes. ACS Cent. Sci. 2018, 4, 1697–1707.
- (70) Ozdemir, S. S.; Buonomenna, M. G.; Drioli, E. Catalytic Polymeric Membranes: Preparation and Application. *Appl. Catal., A* **2006**, 307, 167–183.
- (71) Le, T. X. H.; Haflich, H.; Shah, A. D.; Chaplin, B. P. Energy-Efficient Electrochemical Oxidation of Perfluoroalkyl Substances Using a Ti4O7 Reactive Electrochemical Membrane Anode. *Environ. Sci. Technol. Lett.* **2019**, *6*, 504–510.
- (72) Dioos, B. M. L.; Vankelecom, I. F. J.; Jacobs, P. A. Aspects of Immobilisation of Catalysts on Polymeric Supports. *Adv. Synth. Catal.* **2006**, 348, 1413–1446.
- (73) Puglisi, A.; Benaglia, M.; Chiroli, V. Stereoselective Organic Reactions Promoted by Immobilized Chiral Catalysts in Continuous Flow Systems. *Green Chem.* **2013**, *15*, 1790–1813.
- (74) Lewis, S. R.; Datta, S.; Gui, M.; Coker, E. L.; Huggins, F. E.; Daunert, S.; Bachas, L.; Bhattacharyya, D. Reactive Nanostructured Membranes for Water Purification. *Proc. Natl. Acad. Sci. U. S. A.* **2011**, 108, 8577–8582.
- (75) Chen, Y.; Gao, P.; Summe, M. J.; Phillip, W. A.; Wei, N. Biocatalytic Membranes Prepared by Inkjet Printing Functionalized Yeast Cells onto Microfiltration Substrates. *J. Membr. Sci.* **2018**, *550*, 91–100.
- (76) Dong, J.; Bruening, M. L. Functionalizing Microporous Membranes for Protein Purification and Protein Digestion. *Annu. Rev. Anal. Chem.* **2015**, *8*, 81–100.
- (77) Dong, J.; Ning, W.; Liu, W.; Bruening, M. L. Limited Proteolysis in Porous Membrane Reactors Containing Immobilized Trypsin. *Analyst* **2017**, *142*, 2578–2586.

- (78) Guo, W.; Ngo, H.-H.; Li, J. A Mini-review on Membrane Fouling. *Bioresour. Technol.* **2012**, 122, 27–34.
- (79) Ostuni, E.; Chapman, R. G.; Holmlin, R. E.; Takayama, S.; Whitesides, G. M. A Survey of Structure—Property Relationships of Surfaces that Resist the Adsorption of Protein. *Langmuir* **2001**, *17*, 5605–5620.
- (80) Chang, Y.; Chen, S.; Zhang, Z.; Jiang, S. Highly Protein-resistant Coatings from Well-defined Diblock Copolymers Containing Sulfobetaines. *Langmuir* **2006**, *22*, 2222–2226.
- (81) Yue, W.-W.; Li, H.-J.; Xiang, T.; Qin, H.; Sun, S.-D.; Zhao, C.-S. Grafting of Zwitterion from Polysulfone Membrane via Surface-initiated ATRP with Enhanced Antifouling Property and Biocompatibility. *J. Membr. Sci.* **2013**, *446*, 79–91.
- (82) Bengani, P.; Kou, Y.; Asatekin, A. Zwitterionic Copolymer Self-assembly for Fouling Resistant, High Flux Membranes with Size-based Small Molecule Selectivity. *J. Membr. Sci.* **2015**, 493, 755–765.
- (83) Zhang, R.; Liu, Y.; He, M.; Su, Y.; Zhao, X.; Elimelech, M.; Jiang, Z. Antifouling Membranes for Sustainable Water Purification: Strategies and Mechanisms. *Chem. Soc. Rev.* **2016**, 45, 5888–5924.
- (84) Welch, M. E.; Ober, C. K. Responsive and Patterned Polymer Brushes. J. Polym. Sci., Part B: Polym. Phys. 2013, 51, 1457-1472.
- (85) Discekici, E. H.; Pester, C. W.; Treat, N. J.; Lawrence, I.; Mattson, K. M.; Narupai, B.; Toumayan, E. P.; Luo, Y.; McGrath, A. J.; Clark, P. G.; de Alaniz, J. R.; Hawker, C. J. Simple Benchtop Approach to Polymer Brush Nanostructures Using Visible-Light-Mediated Metal-Free Atom Transfer Radical Polymerization. *ACS Macro Lett.* **2016**, *5*, 258–262.
- (86) Lang, K.; Chin, J. W. Bioorthogonal Reactions for Labeling Proteins. ACS Chem. Biol. 2014, 9, 16–20.
- (87) Saito, F.; Noda, H.; Bode, J. W. Critical Evaluation and Rate Constants of Chemoselective Ligation Reactions for Stoichiometric Conjugations in Water. *ACS Chem. Biol.* **2015**, *10*, 1026–1033.
- (88) Rodionov, V. O.; Fokin, V. V.; Finn, M. G. Mechanism of the Ligand-Free Cu I -Catalyzed Azide—Alkyne Cycloaddition Reaction. *Angew. Chem., Int. Ed.* **2005**, *44*, 2210—2215.
- (89) Cramer, N. B.; Reddy, S. K.; O'Brien, A. K.; Bowman, C. N. Thiol-Ene Photopolymerization Mechanism and Rate Limiting Step Changes for Various Vinyl Functional Group Chemistries. *Macromolecules* **2003**, *36*, 7964–7969.
- (90) Kamcev, J.; Paul, D. R.; Freeman, B. D. Ion Activity Coefficients in Ion Exchange Polymers: Applicability of Manning's Counterion Condensation Theory. *Macromolecules* **2015**, *48*, 8011–8024.
- (91) Weidman, J. L.; Mulvenna, R. A.; Boudouris, B. W.; Phillip, W. A. Nanostructured Membranes from Triblock Polymer Precursors as High Capacity Copper Adsorbents. *Langmuir* **2015**, *31*, 11113–11123.
- (92) Freger, V. Kinetics of Film Formation by Interfacial Polycondensation. *Langmuir* **2005**, *21*, 1884–1894.
- (93) Nowbahar, A.; Mansard, V.; Mecca, J. M.; Paul, M.; Arrowood, T.; Squires, T. M. Measuring Interfacial Polymerization Kinetics Using Microfluidic Interferometry. J. Am. Chem. Soc. 2018, 140, 3173–3176.
- (94) Nuxoll, E. E.; Cussler, E. L. The Third Parameter in Reactive Barrier Films. *AIChE J.* **2005**, *51*, 456–463.
- (95) Chen, T.; Amin, I.; Jordan, R. Patterned Polymer Brushes. *Chem. Soc. Rev.* **2012**, *41*, 3280–3296.
- (96) Hoffman, J. R.; Mikes, A.; Gao, F.; Phillip, W. A. Controlled Post-Assembly Functionalization of Mesoporous Copolymer Membranes Informed by Fourier Transform Infrared Spectroscopy. *ACS Appl. Polym. Mater.* **2019**, *1*, 2120–2130.
- (97) Hoffman, J. R.; Phillip, W. A. Dual-Functional Nanofiltration Membranes Exhibit Multifaceted Ion Rejection and Antifouling Performance. *ACS Appl. Mater. Interfaces* **2020**, *12*, 19944–19954.
- (98) Goldfeld, D. J.; Silver, E. S.; Radlauer, M. R.; Hillmyer, M. A. Synthesis and Self-Assembly of Block Polyelectrolyte Membranes through a Mild, 2-in-1 Postpolymerization Treatment. *ACS Appl. Polym. Mater.* **2020**, *2*, 817–825.
- (99) Fultz, B. A.; Terlier, T.; Dunoyer de Segonzac, B.; Verduzco, R.; Kennemur, J. G. Nanostructured Films of Oppositely Charged Domains from Self-Assembled Block Copolymers. *Macromolecules* **2020**, *53*, 5638–5648.

- (100) Yang, H. C.; Xie, Y.; Hou, J.; Cheetham, A. K.; Chen, V.; Darling, S. B. Janus Membranes: Creating Asymmetry for Energy Efficiency. *Adv. Mater.* **2018**, *30*, 1801495.
- (101) Tian, X.; Jin, H.; Sainio, J.; Ras, R. H. A.; Ikkala, O. Droplet and Fluid Gating by Biomimetic Janus Membranes. *Adv. Funct. Mater.* **2014**, 24, 6023–6028.
- (102) Waldman, R. Z.; Yang, H. C.; Mandia, D. J.; Nealey, P. F.; Elam, J. W.; Darling, S. B. Janus Membranes via Diffusion-Controlled Atomic Layer Deposition. *Adv. Mater. Interfaces* **2018**, *5*, 1800658.
- (103) Yang, H. C.; Waldman, R. Z.; Wu, M. B.; Hou, J.; Chen, L.; Darling, S. B.; Xu, Z. K. Dopamine: Just the Right Medicine for Membranes. *Adv. Funct. Mater.* **2018**, 28, 1705327.
- (104) Wang, H.; Ding, J.; Dai, L.; Wang, X.; Lin, T. Directional Water-transfer through Fabrics Induced by Asymmetric Wettability. *J. Mater. Chem.* **2010**, *20*, 7938–7940.
- (105) Nie, Z.; Kumacheva, E. Patterning Surfaces with Functional Polymers. *Nat. Mater.* **2008**, *7*, 277–290.
- (106) Pester, C. W.; Narupai, B.; Mattson, K. M.; Bothman, D. P.; Klinger, D.; Lee, K. W.; Discekici, E. H.; Hawker, C. J. Engineering Surfaces through Sequential Stop-Flow Photopatterning. *Adv. Mater.* **2016**, *28*, 9292–9300.
- (107) Li, M.; Fromel, M.; Ranaweera, D.; Rocha, S.; Boyer, C.; Pester, C. W. SI-PET-RAFT: Surface-Initiated Photoinduced Electron Transfer-Reversible Addition—Fragmentation Chain Transfer Polymerization. *ACS Macro Lett.* **2019**, *8*, 374—380.
- (108) Qu, S.; Shi, Y.; Benavides, S.; Hunter, A.; Gao, H.; Phillip, W. A. Copolymer Nanofilters with Charge-Patterned Domains for Enhanced Electrolyte Transport. *Chem. Mater.* **2017**, *29*, 762–772.
- (109) Hones, J.; Muller, P.; Surridge, N. The Technology Behind Glucose Meters: Test Strips. *Diabetes Technol. Ther.* **2008**, *10*, S10–S26.
- (110) Cui, G.; Yoo, J. H.; Yoo, J.; Lee, S. W.; Nam, H.; Cha, G. S. Differential Thick-film Amperometric Glucose Sensor with an Enzyme-immobilized Nitrocellulose Membrane. *Electroanalysis* **2001**, *13*, 224–228.
- (111) Yang, Y.; Zhang, S. F.; Kingston, M. A.; Jones, G.; Wright, G.; Spencer, S. A. Glucose Sensor with Improved Haemocompatibilty. *Biosens. Bioelectron.* **2000**, *15*, 221–227.
- (112) Yeo, L. Y.; Chang, H.-C.; Chan, P. P. Y.; Friend, J. R. Microfluidic Devices for Bioapplications. *Small* **2011**, *7*, 12–48.
- (113) Sassolas, A.; Leca-Bouvier, B. D.; Blum, L. J. DNA Biosensors and Microarrays. *Chem. Rev.* **2008**, *108*, 109–139.
- (114) Song, Y.; Lin, B.; Tian, T.; Xu, X.; Wang, W.; Ruan, Q.; Guo, J.; Zhu, Z.; Yang, C. Recent Progress in Microfluidics-Based Biosensing. *Anal. Chem.* **2019**, *91*, 388–404.
- (115) Yang, Y.; Noviana, E.; Nguyen, M. P.; Geiss, B. J.; Dandy, D. S.; Henry, C. S. Paper-Based Microfluidic Devices: Emerging Themes and Applications. *Anal. Chem.* **2017**, *89*, 71–91.
- (116) Y Yang, M.; Zhang, W.; Yang, J.; Hu, B.; Cao, F.; Zheng, W.; Chen, Y.; Jiang, X. Skiving Stacked Sheets of Paper into Test Paper for Rapid and Multiplexed Assay. *Sci. Adv.* **2017**, *3*, eaao4862.
- (117) Slouka, Z.; Senapati, S.; Chang, H.-C. Microfluidic Systems with Ion-Selective Membranes. *Annu. Rev. Anal. Chem.* **2014**, *7*, 317–335.
- (118) Jia, F.; Narasimhan, B.; Mallapragada, S. Materials-based Strategies for Multi-enzyme Immobilization and Co-localization: A Review. *Biotechnol. Bioeng.* **2014**, *111*, 209–222.
- (119) Logan, T. C.; Clark, D. S.; Stachowiak, T. B.; Svec, F.; Frechet, J. M. J. Photopatterning Enzymes on Polymer Monoliths in Microfluidic Devices for Steady-state Kinetic Analysis and Spatially Separated Multienzyme Reactions. *Anal. Chem.* **2007**, *79*, 6592–6598.
- (120) Chen, Z.; Zhang, J.; Singh, S.; Peltier-Pain, P.; Thorson, J. S.; Hinds, B. J. Functionalized Anodic Aluminum Oxide Membrane-electrode System for Enzyme Immobilization. *ACS Nano* **2014**, *8*, 8104–8112.
- (121) Hou, X. Smart Gating Multi-Scale Pore/Channel-Based Membranes. *Adv. Mater.* **2016**, 28, 7049–64.
- (122) Ma, B.; Ju, X. J.; Luo, F.; Liu, Y. Q.; Wang, Y.; Liu, Z.; Wang, W.; Xie, R.; Chu, L. Y. Facile Fabrication of Composite Membranes with

- Dual Thermo- and pH-Responsive Characteristics. ACS Appl. Mater. Interfaces 2017, 9, 14409–14421.
- (123) Lee, B. Y.; Hyun, S.; Jeon, G.; Kim, E. Y.; Kim, J.; Kim, W. J.; Kim, J. K. Bioinspired Dual Stimuli-Responsive Membranous System with Multiple On-Off Gates. *ACS Appl. Mater. Interfaces* **2016**, 8, 11758–11764.
- (124) Tufani, A.; Ozaydin Ince, G. Protein Gating by Vapor Deposited Janus Membranes. J. Membr. Sci. 2019, 575, 126–134.
- (125) Zhao, X.-P.; Wang, S.-S.; Younis, M. R.; Xia, X.-H.; Wang, C. Thermo and pH Dual Actuating Smart Porous Anodic Aluminum for Controllable Drug Release. *Adv. Mater. Interfaces* **2018**, *5*, 1800185.
- (126) Zhang, Q.; Kang, J.; Xie, Z.; Diao, X.; Liu, Z.; Zhai, J. Highly Efficient Gating of Electrically Actuated Nanochannels for Pulsatile Drug Delivery Stemming from a Reversible Wettability Switch. *Adv. Mater.* **2018**, *30*, 1703323.
- (127) Shaikh, R. P.; Pillay, V.; Choonara, Y. E.; du Toit, L. C.; Ndesendo, V. M.; Bawa, P.; Cooppan, S. A Review of Multi-responsive Membranous Systems for Rate-modulated Drug Delivery. *AAPS PharmSciTech* **2010**, *11*, 441–59.
- (128) Zhang, H.; Hou, X.; Zeng, L.; Yang, F.; Li, L.; Yan, D.; Tian, Y.; Jiang, L. Bioinspired Artificial Single Ion Pump. *J. Am. Chem. Soc.* **2013**, 135, 16102—16110.
- (129) Benavides, S.; Qu, S.; Gao, F.; Phillip, W. A. Polymeric Ion Pumps: Using an Oscillating Stimulus To Drive Solute Transport in Reactive Membranes. *Langmuir* **2018**, *34*, 4503–4514.
- (130) Chen, Z. Q.; Chen, T.; Sun, X. H.; Hinds, B. J. Dynamic Electrochemical Membranes for Continuous Affinity Protein Separation. *Adv. Funct. Mater.* **2014**, 24, 4317–4323.
- (131) Lau, B.; Kedem, O.; Schwabacher, J.; Kwasnieski, D.; Weiss, E. A. An Introduction to Ratchets in Chemistry and Biology. *Mater. Horiz.* **2017**, *4*, 310–318.
- (132) Zhang, Y.; Schatz, G. C. Conical Nanopores for Efficient Ion Pumping and Desalination. *J. Phys. Chem. Lett.* **2017**, *8*, 2842–2848.
- (133) Ardo, S.; Segev, G.; Toma, F. M.; Ager, J. W., III; Kautz, R.; Larson, D. M. Ratchet-based Ion Pumping Membrane Systems. *Intellectual Property*, University of California: Irvine, US 16/907,076, 2020
- (134) Lu, Q.; Tang, Q.; Chen, Z.; Zhao, S.; Qing, G.; Sun, T. Developing an Inositol-Phosphate-Actuated Nanochannel System by Mimicking Biological Calcium Ion Channels. ACS Appl. Mater. Interfaces 2017, 9, 32554–32564.
- (135) Yang, H. C.; Hou, J.; Chen, V.; Xu, Z. K. Janus Membranes: Exploring Duality for Advanced Separation. *Angew. Chem., Int. Ed.* **2016**, *55*, 13398–13407.
- (136) Li, H. N.; Yang, J.; Xu, Z. K. Asymmetric Surface Engineering for Janus Membranes. *Adv. Mater. Interfaces* **2020**, *7*, 1902064.
- (137) Cheng, L. J.; Chang, H. C. Microscale pH Regulation by Splitting Water. *Biomicrofluidics* **2011**, *5*, 46502–46508.
- (138) Balster, J.; Sumbharaju, R.; Srikantharajah, S.; Pünt, I.; Stamatialis, D. F.; Jordan, V.; Wessling, M. Asymmetric Bipolar Membrane: A Tool to Improve Product Purity. *J. Membr. Sci.* **2007**, 287, 246–256.
- (139) Balster, J.; Srinkantharajah, S.; Sumbharaju, R.; Pünt, I.; Lammertink, R. G. H.; Stamatialis, D. F.; Wessling, M. Tailoring the Interface Layer of the Bipolar Membrane. *J. Membr. Sci.* **2010**, *365*, 389–398
- (140) Oener, S. Z.; Foster, M. J.; Boettcher, S. W. Accelerating Water Dissociation in Bipolar Membranes and for Electrocatalysis. *Science* **2020**, eaaz1487.
- (141) Shen, C.; Wycisk, R.; Pintauro, P. N. High Performance Electrospun Bipolar Membrane with a 3D Junction. *Energy Environ. Sci.* **2017**, *10*, 1435–1442.
- (142) Jordan, M. L.; Valentino, L.; Nazyrynbekova, N.; Palakkal, V. M.; Kole, S.; Bhattacharya, D.; Lin, Y. J.; Arges, C. G. Promoting Watersplitting in Janus Bipolar Ion-exchange Resin Wafers for Electrodeionization. *Mol. Syst. Des. Eng.* **2020**, *5*, 922–935.
- (143) White, W.; Sanborn, C. D.; Fabian, D. M.; Ardo, S. Conversion of Visible Light into Ionic Power Using Photoacid-Dye-Sensitized Bipolar Ion-Exchange Membranes. *Joule* **2018**, *2*, 94–109.

- (144) Lin, F. D.; Lonergan, M. C. Semiconducting Bipolar Membranes: Photochemical Salt Pumps. *Acs Appl. Energy Mater.* **2020**, 3, 4103–4107.
- (145) Siwy, Z. S. Ion-Current Rectification in Nanopores and Nanotubes with Broken Symmetry. *Adv. Funct. Mater.* **2006**, *16*, 735–746.
- (146) Li, R.; Fan, X.; Liu, Z.; Zhai, J. Smart Bioinspired Nanochannels and their Applications in Energy-Conversion Systems. *Adv. Mater.* **2017**, *29*, 1702983.
- (147) Zhao, J.; Zhao, X.; Jiang, Z.; Li, Z.; Fan, X.; Zhu, J.; Wu, H.; Su, Y.; Yang, D.; Pan, F.; Shi, J. Biomimetic and Bioinspired Membranes: Preparation and Application. *Prog. Polym. Sci.* **2014**, *39*, 1668–1720.
- (148) Huang, X.; Kong, X.-Y.; Wen, L.; Jiang, L. Bioinspired Ionic Diodes: From Unipolar to Bipolar. *Adv. Funct. Mater.* **2018**, 28, 1801079.
- (149) Zhang, Q.; Zhang, Z.; Zhou, H.; Xie, Z.; Wen, L.; Liu, Z.; Zhai, J.; Diao, X. Redox Switch of Ionic Transport in Conductive Polypyrrole-engineered Unipolar Nanofluidic Diodes. *Nano Res.* **2017**, *10*, 3715–3725.
- (150) Zhang, Z.; Huang, X.; Qian, Y.; Chen, W.; Wen, L.; Jiang, L. Engineering Smart Nanofluidic Systems for Artificial Ion Channels and Ion Pumps: From Single-Pore to Multichannel Membranes. *Adv. Mater.* **2020**, *32*, 1904351.
- (151) Gao, J.; Guo, W.; Feng, D.; Wang, H.; Zhao, D.; Jiang, L. High-performance Ionic Diode Membrane for Salinity Gradient Power Generation. *J. Am. Chem. Soc.* **2014**, *136*, 12265–12272.
- (152) Yip, N. Y.; Brogioli, D.; Hamelers, H. V.; Nijmeijer, K. Salinity Gradients for Sustainable Energy: Primer, Progress, and Prospects. *Environ. Sci. Technol.* **2016**, *50*, 12072–12094.
- (153) Wang, S.; Yang, X.; Wu, F.; Min, L.; Chen, X.; Hou, X. Inner Surface Design of Functional Microchannels for Microscale Flow Control. *Small* **2020**, *16*, 1905318.
- (154) Li, X.; Zhai, T.; Gao, P.; Cheng, H.; Hou, R.; Lou, X.; Xia, F. Role of Outer Surface Probes for Regulating Ion Gating of Nanochannels. *Nat. Commun.* **2018**, *9*, 40.
- (155) Acar, E. T.; Buchsbaum, S. F.; Combs, C.; Fornasiero, F.; Siwy, Z. S. Biomimetic Potassium Selective Nanopores. *Sci. Adv.* **2019**, *5*, eaav2568.
- (156) Davidson, S. M.; Wessling, M.; Mani, A. On the Dynamical Regimes of Pattern-Accelerated Electroconvection. *Sci. Rep.* **2016**, *6*, 22505
- (157) Roghmans, F.; Evdochenko, E.; Stockmeier, F.; Schneider, S.; Smailji, A.; Tiwari, R.; Mikosch, A.; Karatay, E.; Kühne, A.; Walther, A.; Mani, A.; Wessling, M. 2D Patterned Ion-Exchange Membranes Induce Electroconvection. *Adv. Mater. Interfaces* **2019**, *6*, 1801309.
- (158) Gao, P.; Hunter, A.; Summe, M. J.; Phillip, W. A. A Method for the Efficient Fabrication of Multifunctional Mosaic Membranes by Inkjet Printing. ACS Appl. Mater. Interfaces 2016, 8, 19772—19779.
- (159) Summe, M. J.; Sahoo, S. J.; Whitmer, J. K.; Phillip, W. A. Salt Permeation Mechanisms in Charge-patterned Mosaic Membranes. *Mol. Syst. Des. Eng.* **2018**, *3*, 959–969.
- (160) Gao, F.; Hunter, A.; Qu, S.; Hoffman, J. R.; Gao, P.; Phillip, W. A. Interfacial Junctions Control Electrolyte Transport through Charge-Patterned Membranes. *ACS Nano* **2019**, *13*, 7655–7664.
- (161) Wang, C.; Brown, G. O.; Burris, D. L.; Korley, L. T. J.; Epps, T. H. Coating Architects: Manipulating Multiscale Structures To Optimize Interfacial Properties for Coating Applications. *ACS Appl. Polym. Mater.* **2019**, *1*, 2249–2266.
- (162) Monroe, J. I.; Shell, M. S. Computational Discovery of Chemically Patterned Surfaces that Effect Unique Hydration Water Dynamics. *Proc. Natl. Acad. Sci. U. S. A.* **2018**, *115*, 8093–8098.